JOURNAL OF SOLID STATE CHEMISTRY 106, 317–329 (1993)

Additional Oxygen Ordering in "$La_2NiO_{4.25}$" ($La_8Ni_4O_{17}$). I. Electron and Neutron Diffraction Study

A. DEMOURGUES, F. WEILL, B. DARRIET, A. WATTIAUX, J. C. GRENIER, P. GRAVEREAU, AND M. POUCHARD

Laboratoire de Chimie du Solide du CNRS, Université de Bordeaux I, 351, Cours de la Libération, 33405 Talence Cedex, France

Received June 15, 1992; in revised form March 25, 1993; Accepted March 29, 1993

A new material with the composition $La_2NiO_{4.25}$ exhibiting a large additional oxygen amount with respect to the K_2NiF_4-type structure has been prepared using an electrochemical process. A monoclinic unit cell (C-centered) has been determined by TEM. This monoclinic unit cell is four times bigger than the average orthorhombic unit cell and the refined parameters are $a = 13.832$ Å, $b = 10.930$ Å, $c = 10.912$ Å, $\beta = 113.31°$. The structure has been determined from neutron powder-diffraction data at 300 and 9 K. The space group is $C2$. In this space group the site of the additional oxygen atoms is fully occupied. The composition $La_2NiO_{4.25}$ corresponds to a define compound: $La_8Ni_4O_{17}$.

Introduction

A renewed interest has been found in the study of oxides with K_2NiF_4-type structure since superconductivity has been pointed out in $La_2CuO_{4+\delta}$ (*1*). Superconducting properties of La_2CuO_4 arises from the presence of holes in the CuO_2 planes, which can be obtained for instance by oxygen overstoichiometry (*1*, *2*).

The nature and the location of the additional oxygen atoms in such a compact structure have raised many controversies (*3*, *4*).

In this way, the homologous compound La_2NiO_4, whose content of excess oxygen can reach higher values ($\delta \approx 0.20$), was also investigated (*5*, *6*).

Neutron diffraction studies on both compounds showed that the additional oxygen is located in an interstitial site between two (LaO) layers, occupying a random position (*5*, *7*).

More recently, electron diffraction studies (*8–10*) of $La_2NiO_{4+\delta}$ gave evidence of various commensurate and incommensurate superstructures that were attributed to the additional oxygen ordering.

In previous works we reported that the use of electrochemical oxidation in alkaline solution allows to prepare bulky oxidized compounds (*11*); more especially, for $La_2NiO_{4+\delta}$, the amount of over-stoichiometric oxygen could be increased compared to more usual synthesis routes since we obtained compositions up to $La_2NiO_{4.25}$ (*12*).

In this paper we report the determination of the structure of the latter compound by means of electron and neutron powder diffraction. The ordering of the additional oxygen atoms will be described.

I. Preparation and Experimental

The method of preparation of $La_2NiO_{4.25}$ was described in detail in a previous work (*12*). This material was obtained using electrochemical oxidation of $La_2NiO_{4.14}$ prepared by a solid state reaction in air.

For neutron diffraction experiments, the electrochemical oxidation was carried out on a 10-g ceramic (32 mm diameter and 2

0022-4596/93 $5.00

mm thickness) of $La_2NiO_{4.14}$ during 15 days under an anodic potential of 600 mV.

The chemical analysis of the final material, carried out by means of fluorine selective electrodes (lanthanum), atomic absorption (nickel), iodometric titration, Mohr's salt method (formally trivalent nickel or hole concentration) and TGA measurements (oxygen) leads to be following chemical formula: $La_2NiO_{4.25}$.

The powder X-ray diffraction patterns can be indexed in the *Fmmm* space group with the following unit cell parameters: a = 5.460 Å, b = 5.456 Å, c = 12.701 Å.

TEM observations were performed with a JEOL 2000 FX electron microscope equipped with a cryogenic double tilt specimen stage. Experiments were achieved at 100 K in order to prevent a modification of the sample caused by the electron beam under high vacuum. The material was ground in ethanol and crystallites were deposited on a holey carbon support film. The electron diffraction patterns were obtained by selected area diffraction. Neutron diffraction experiments were performed at the I.L.L. neutron source using the high resolution diffractometer D2B. The sample holder was made of vanadium and the used wavelength was $\lambda = 1.594$ Å. The diffractograms ($6° \leq 2\theta \leq 155°$) were recorded at 298 K and 9 K and the data collected for Rietveld structure refinement.

II. Electron Microscopy Study

The electron microscopy study of $La_2NiO_{4.25}$ has revealed the existence of a superstructure: the electron diffraction patterns (Fig. 1) obviously show additional spots that cannot be indexed using the *Fmmm* cell. This superstructure does not exist in La_2NiO_4 as shown in Fig. 2. We can then assume that these additional spots result from a structural ordering due to the presence of oxygen excess in $La_2NiO_{4.25}$.

From several electron diffraction patterns (Fig. 1) obtained by successive rotations of the specimen, the reciprocal lattice of $La_2NiO_{4.25}$ can be built up.

Figure 3 is a partial reconstitution of the reciprocal space, the orthorhombic cell is outlined and the labelling of the superstructure spots, using the *Fmmm* cell, is indicated.

To describe the whole reciprocal space a triclinic cell has to be used as elementary cell. The relationship between the orthorhombic cell and this triclinic cell is

$$\begin{pmatrix} a^* \\ b^* \\ c^* \end{pmatrix}_{tr} = \begin{pmatrix} 0 & \frac{1}{2} & \frac{1}{2} \\ \frac{1}{2} & \frac{1}{2} & -\frac{1}{2} \\ \frac{1}{2} & \frac{1}{2} & \frac{1}{2} \end{pmatrix} \begin{pmatrix} a^* \\ b^* \\ c^* \end{pmatrix}_o .$$

Its parameters, calculated from the X-ray parameters, are

$$a = 13.81 \text{ Å} \quad b = 8.81 \text{ Å} \quad c = 8.81 \text{ Å}$$
$$\alpha = 76.67° \quad \beta = 122.67° \quad \gamma = 122.67°$$
$$V_{tr} = 2V_o .$$

According to Chaillout *et al.* (*7*) and Jorgensen *et al.* (*5*), it is now well known that the additional oxygen atoms are located in interstitial sites between two adjacent LaO layers, and are surrounded by four lanthanum atoms and four oxygen atoms that are slightly displaced from their (0, 0, z) 8*i* positions (space group: *Fmmm*) (Fig. 4).

On the basis of this location and of the observed reciprocal space we have already proposed (*9*) a structural model describing the ordering of these additional oxygen atoms.

A further investigation should propose a multiple cell of the triclinic cell that would describe the structure with a higher symmetry.

Hiroi *et al.* (*8*) already suggested an orthorhombic supercell ($2a \times 3b \times 6c$) but such a multiple cell is inconsistent with the observed reciprocal space of our materials. Actually this multiple cell involves a large number of systematic extinctions without any cristallographical meaning. For instance, in the c^* direction the Hiroi supercell implies that g_{001} is divided by 6,

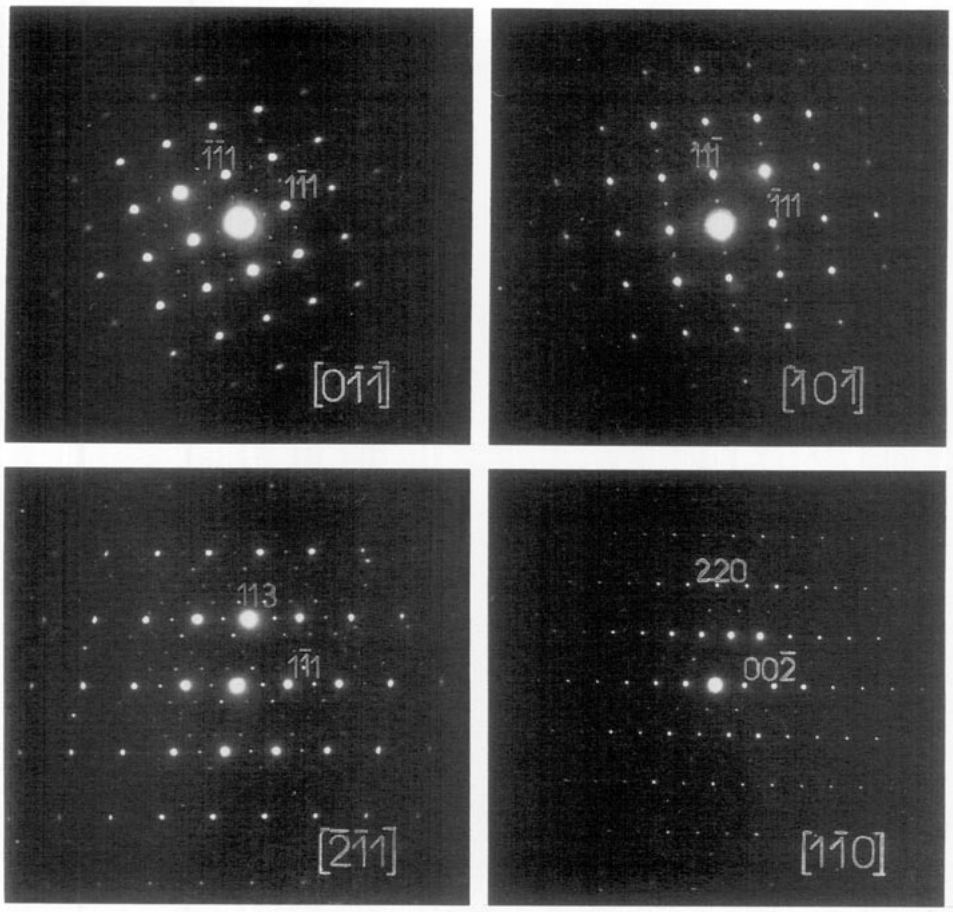

FIG. 1. Electron diffraction patterns of $La_2NiO_{4.25}$.

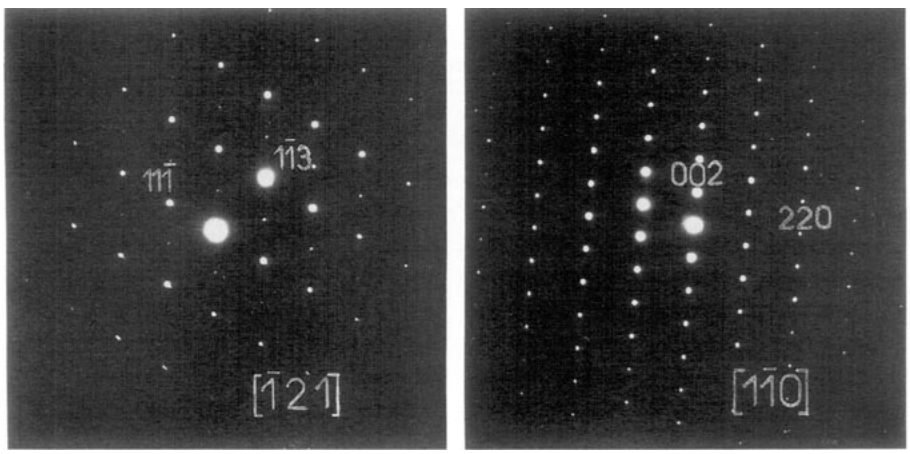

FIG. 2. Electron diffraction patterns of La_2NiO_4.

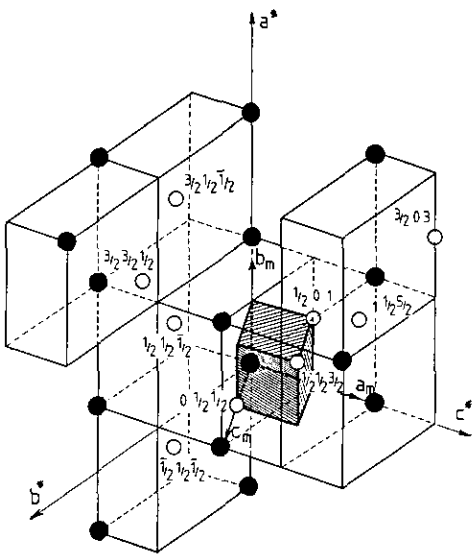

FIG. 3. Partial reconstitution of the reciprocal space of $La_2NiO_{4.25}$. The *Fmmm* space group is used to label the superstructure spots (open circles). Both the orthorhombic cell (—) and the monoclinic cell (hatched cell) are shown.

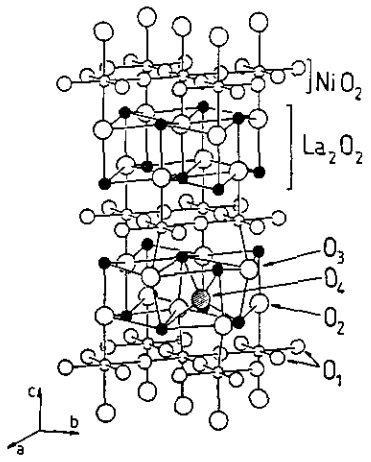

○ Nickel ● Lanthanum
○ Oxygen in the NiO_2 layers
○ Oxygen in the NaCl-type double LaO layers
◉ Interstitial oxygen

FIG. 4. Idealized structure of $La_2NiO_{4+\delta}$ (*Fmmm* space group) according to Jorgensen *et al.* (5).

whereas we do not observed any superstructure spots along this direction.

From our observations the shortest distance, in the reciprocal space, is along $[022]_o^*$ which have led us to build the triclinic cell by choosing a_{tr}^* along this direction.

Furthermore in a previous work (*9*) we suggested that this direction is the limiting position of the modulation vector characterizing the incommensurate superstructure of the $La_2NiO_{4+\delta}$ phases with $0.17 < \delta < 0.25$.

We then based the search for a multiple cell using this direction as the first basis vector.

As second basis vector we chose a linear combination of b_{tr}^* and c_{tr}^*. As a matter of fact the vectorial sum $b_{tr}^* + c_{tr}^*$ lies along the main direction a^* of the orthorhombic unit cell. Obviously the angle between [022]* and [100]* is 90°, but it is impossible to find a third crystallographic direction perpendicular to both [022]* and [100]*. Then, the symmetry of the multiple cell cannot be orthorhombic. For this reason we chose as third basis vector of the multiple cell, the c^* orthorhombic vector. Consequently the symmetry of the multiple cell based on these three vectors is monoclinic.

The vectorial relationship in the reciprocal space between this monoclinic cell and the orthorhombic-type cell is then

$$\begin{pmatrix} a^* \\ b^* \\ c^* \end{pmatrix}_m = \underbrace{\begin{pmatrix} 0 & 0 & 1 \\ \frac{1}{2} & 0 & 0 \\ 0 & \frac{1}{2} & \frac{1}{2} \end{pmatrix}}_{P} \begin{pmatrix} a^* \\ b^* \\ c^* \end{pmatrix}_o ,$$

which corresponds in the direct space to unit cell parameters close to

$$a = 13.80 \text{ Å } b = 10.92 \text{ Å } c = 10.91 \text{ Å}$$

$$\beta = 113.2°$$

$$V_m = 2V_{tr} = 4V_o .$$

The Miller indices in the monoclinic cell can be deduced from those of the orthorhombic cell using the inverse matrix: $Q = P^{-1}$.

So, the monoclinic indexation leads to re-

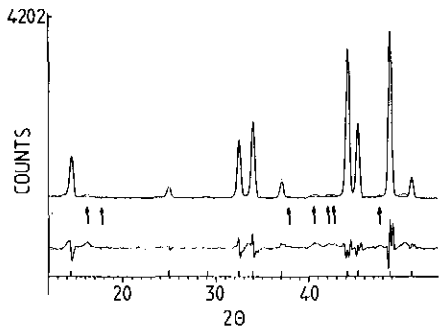

FIG. 5. Portion of the Rietveld refinement profile of $La_2NiO_{4.25}$ in the *Fmmm* space group. Experimental (···), calculated (—), and difference patterns are plotted.

flection condition $h_m + k_m = 2n$ which characterizes a C-centered Bravais lattice.

III. Neutron Diffraction

In a previous work, preliminary refinements for $La_2NiO_{4.25}$ were achieved assuming the *Fmmm* orthorhombic space group as previously suggested by Jorgensen *et al.* (*5*) for $La_2NiO_{4.18}$. The O(4) additional oxygen atoms (Fig. 4) were located at ($\frac{1}{4}$, $\frac{1}{4}$, $z \approx \frac{1}{4}$) (16*j* Wyckoff position), while the apical oxygen atoms were split into two different positions:

- the first one, O(2) located at (0, 0, *z*) (8*i* Wyckoff position) is in the normal position.
- the second one, O(3), [(*x*, *y*, *z*), 32*p* Wyckoff position] is shifted from the normal position due to the presence of the additional oxygen atom.

The refinement leads to an excellent agreement with the $La_2NiO_{4.25}$ composition determined by chemical analysis. In addition these results show that the presence of an oxygen atom in the O(4) site displaces four oxygen atoms from their O(2) position towards the O(3) site. A portion ($6° \leq 2\theta \leq 40°$) of the Rietveld refinement profile is plotted in Fig. 5.

It is worthwhile to emphasize that small experimental peaks are not indexed in the *Fmmm* or even in the *Bmab* space groups. On the other hand, these peaks cannot correspond to magnetic reflections because the oxidized samples ($\delta > 0.10$) do not magnetically order at least for temperatures as low as 1.5 K (*13*). In addition, the magnetic susceptibility of $La_2NiO_{4.25}$ follows a Curie–Weiss law in the $4\text{ K} < T < 170\text{ K}$ temperature range ($C \approx 0.33$ emu.K) (*14*).

The above electron diffraction investigation has demonstrated that the true cell is likely different from the orthorhombic *Fmmm* unit cell. Indeed, using the C monoclinic cell determined by electron diffraction, the small peaks can be indexed (Table I). This indexation suggests that the *Cc* and *C2/c* space groups are to be ruled out.

Assuming that the additional oxygen atoms are located in the 16*j* Wyckoff position ($\frac{1}{4}$, $\frac{1}{4}$, *z*) of the *Fmmm* space group, three kinds of ordering of additional oxygen atoms corresponding to the three space groups (*C2*, *Cm*, and *C2/m*) can be distinguished. The locations of the four additional oxygen atoms in the various groups are represented in Fig. 6.

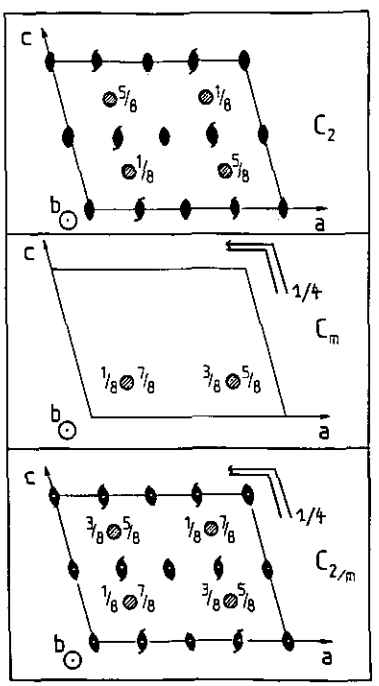

FIG. 6. Ordering of additional oxygen atoms corresponding to the *C2*, *Cm*, and *C2/m* space groups.

TABLE I

NEUTRON POWDER DIFFRACTION DATA FOR $La_2NiO_{4.25}$ INDEXED IN THE MONOCLINIC AND ORTHORHOMBIC UNIT CELLS AT 298 K

hkl Monoclinic	*hkl* Orthorhombic	d_{hkl}	I_{obs}
200	002	6.3517	471
111	$\frac{1}{2}\frac{1}{2}\frac{3}{2}$	5.7035	61
$20\bar{2}$	011	5.0159	
$00\bar{2}$		5.0109	13
$31\bar{1}$	$\frac{1}{2}\frac{\bar{1}}{2}\frac{5}{2}$	4.2469	4
$22\bar{2}$		3.6953	
$02\bar{2}$	111	3.6934	119
022		3.6934	
400	004	3.1759	3
$42\bar{2}$	113	2.8545	
$22\bar{2}$		2.8518	581
040	200	2.7325	
$20\bar{4}$	020	2.7281	788
$13\bar{3}$	$\frac{3}{2}\frac{3}{2}\frac{1}{2}$	2.5608	7
240	202	2.5101	
404		2.5079	
004	022	2.5054	217
$51\bar{3}$	$\frac{1}{2}\frac{\bar{3}}{2}\frac{7}{2}$	2.5027	
331	$\frac{3}{2}\frac{1}{2}\frac{7}{2}$	2.5022	
$33\bar{3}$	$\frac{3}{2}\frac{\bar{3}}{2}\frac{3}{2}$	2.4636	6
$22\bar{4}$	$1\bar{2}0$	2.4409	13
$60\bar{2}$	$0\bar{1}5$	2.3045	10
133	$\frac{3}{2}\frac{3}{2}\frac{5}{2}$	2.2954	20
$60\bar{3}$	$0\frac{\bar{3}}{2}\frac{3}{2}$	2.2317	13
511	$\frac{1}{2}\frac{1}{2}\frac{11}{2}$	2.2123	14
$53\bar{1}$	$\frac{3}{2}\frac{\bar{1}}{2}\frac{9}{2}$	2.1867	
313	$\frac{1}{2}\frac{3}{2}\frac{9}{2}$	2.1838	17
$62\bar{2}$	115	2.1234	
$42\bar{2}$		2.1215	841
600	006	2.1173	
$44\bar{2}$	$2\bar{1}3$	2.1168	668
242	211	2.1157	
440	204	2.0713	
$60\bar{4}$	024	2.0708	709
204		2.0680	
$35\bar{1}$	$\frac{5}{2}\frac{1}{2}\frac{5}{2}$	1.9751	
620	106	1.9743	23
$51\bar{5}$	$\frac{1}{2}\frac{\bar{5}}{2}\frac{5}{2}$	1.9734	

It is important to mention that for the centrosymmetric $C2/m$ space group, the additional oxygen site occupancy in $La_2NiO_{4.25}$ is equal to 50%, while it is equal to 100% for the noncentrosymmetric $C2$ or Cm space groups.

For the latter groups we can consider that the $La_2NiO_{4.25}$ composition corresponds to a definite compound $La_8Ni_4O_{17}$.

The atomic coordinates in the monoclinic cell have been calculated starting from those of the orthorhombic unit cell (*Fmmm* space group) using the matrix relationship (P matrix). The general positions of atoms are reported in Table II. The values of the Debye–Waller factors were set up to be identical for all lanthanum atoms on the one hand and for all nickel atoms on the other hand. Various temperature factors corresponding to O_z apical oxygen atoms to O_{xy} oxygen atoms belonging to (NiO_2) planes, and to O_i additional oxygen atoms have been considered. The five Debye–Waller factors were refined as well as the atomic positions.

It should be mentioned again that all diffraction-line peaks have been taken into account in the three monoclinic refinements (for instance the $(111)_m$, $(1\bar{1}1)_m$ corresponding to the $(\frac{1}{2}, \frac{1}{2}, \frac{3}{2})_o$ and $(\frac{\bar{1}}{2}, \frac{1}{2}, \frac{3}{2})_o$, arrows ↑ in Fig. 5 and Fig. 7).

The reliability factors and the number of refined parameters are given in Table III. The lowest values are obtained for the $C2$ space group. In spite of the high number of refined parameters, this group seems to be the most likely. Additional calculations were performed in order to corroborate this assumption.

1. Reduced Reliability Factors

The reduced reliability factors, R_I^*, calculated by taking into account only the small diffraction line peaks (arrows in Fig. 5) and characteristic of interstitial oxygen ordering are reported in Table IV with the observed and calculated intensities at 9 K. Although high values are obtained (only few weak reflections) this calculation suggests that C_2 and Cm are the most representative space groups for the ordering of the additional oxygen.

2. Hamilton's Test

Moreover, the Hamilton's R factor ratio test (*15*) makes it possible to decide whether

TABLE II

GENERAL POSITIONS OF ATOMS IN $La_2NiO_{4.25}$ CORRESPONDING TO THE VARIOUS SPACE GROUPS: *C*2, *Cm*, *C*2/*m*

Space group	Atom	Number of atoms whose coordinates are refined	Multiplicity	Wyckoff positions
*C*2	La	8	4*c*	*x*, *y*, *z*
	Ni	2	2*a*	0, *y*, 0
		2	2*b*	0, *y*, ½
		2	4*c*	*x*, *y*, *z*
	O_{xy}	8	4*c*	*x*, *y*, *z*
	O_z	8	4*c*	*x*, *y*, *z*
	O_I	1	4*c*	*x*, *y*, *z*
Cm	La	8	2*a*	*x*, 0, *z*
		4	4*c*	*x*, *y*, *z*
	Ni	4	2*a*	*x*, 0, *z*
		2	4*c*	*x*, *y*, *z*
	O_{xy}	8	4*c*	*x*, *y*, *z*
	O_z	8	2*a*	*x*, 0, *z*
		4	4*c*	*x*, *y*, *z*
	O_I	1	4*c*	*x*, *y*, *z*
*C*2/*m*	La	4	4*i*	*x*, 0, *z*
		2	8*j*	*x*, *y*, *z*
	N_i	1	2*a*	0, 0, 0
		1	2*b*	0, ½, 0
		1	2*c*	0, 0, ½
		1	2*d*	0, ½, ½
		1	8*j*	*x*, *y*, *z*
	O_{xy}	4	8*j*	*x*, *y*, *z*
	O_z	4	4*i*	*x*, 0, *z*
		8	8*j*	*x*, *y*, *z*
	O_I	1	8*j* (50%)	*x*, *y*, *z*

TABLE III

RELIABILITY FACTORS (R_p, R_{wp} AND R_I) OBTAINED IN *Fmmm*, *C*2, *Cm*, AND *C*2/*m*-STRUCTURE REFINEMENTS

	Fmmm	*C*2		*Cm*		*C*2/*m*	
	298 K	298 K	9 K	298 K	9 K	298 K	9 K
Number of refined parameters	28	105		117		68	
Reliability factors							
R_p %[a]	4.51	3.74	4.23	3.80	4.31	3.93	4.40
R_{wp} %[b]	5.78	4.86	5.34	4.94	5.47	5.12	5.58
R_I %[c]	6.27	5.69	6.42	5.96	6.82	6.30	6.94
R_{exp} %[d]	1.72	1.70	1.56	1.70	1.56	1.71	1.57

[a] $R_p = 100\ \Sigma_i\ [y_i\ (\text{obs}) - (1/c)\ y_i\ (\text{calc})]/\Sigma_i\ y_i(\text{obs})$ (profile).

[b] $R_{wp} = 100\ \sqrt{\Sigma_i\ w_i[\ y_i(\text{obs}) - (1/c)\ y_i(\text{calc})]^2/\Sigma_i\ w_i[\ y_i(\text{obs})]^2}$ (weighted profile).

[c] $R_I = 100\ \Sigma_i\ [I(\text{obs}) - (1/c)\ I(\text{cal})]/\Sigma_i\ I(\text{obs})$ (Bragg *R*).

[d] $R_{exp} = 100\ \sqrt{(N - P + C)/\Sigma_i\ w_i[\ y_i(\text{obs})]^2}$ (expected *R*).

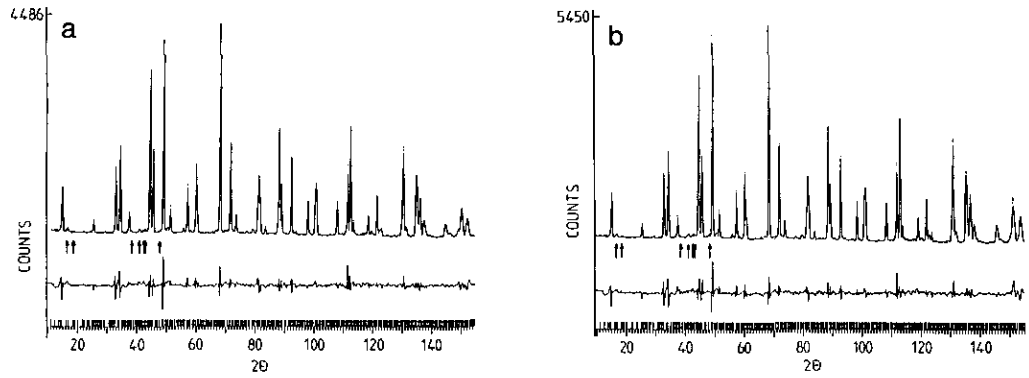

FIG. 7. Portion of the Rietveld refinement profile of $La_8Ni_4O_{17}$ in the C_2 space group at 9 K (a) and 298 K (b). Experimental (···), calculated (—), and difference patterns are plotted.

the addition of parameters (105 refined parameters for the C_2 space group instead of 68 for the C_2/m space group) results in a significant improvement or a significant worsening of the agreement between the observed and calculated neutron diffraction pattern. Relations have been developed by Hamilton which provide significance tests for the experimental $\mathcal{R}$ factor ratio, $\mathcal{R} = \sqrt{R_{wp_1}}/\sqrt{R_{wp_0}}$, where R_{wp_0} and R_{wp_1} are respectively the generalized weighted R factors resulting from an unrestrained least square refinement and a refinement with restraints on some of the parameters. The

TABLE IV

CALCULATED AND OBSERVED INTENSITIES (NEUTRON DIFFRACTION PATTERN OF $La_2NiO_{4.25}$ AT 9 K) CORRESPONDING TO THE SMALL DIFFRACTION LINE PEAKS MENTIONED IN FIG. 5 AND CHARACTERISTIC OF INTERSTITIAL OXYGEN ORDERING

Diffraction line peaks	*hkl* mono	*hkl* orth	*C*2 9 K		*Cm* 9 K		*C*2/*m* 9 K	
			I_{calc}	I_{obs}	I_{calc}	I_{obs}	I_{calc}	I_{obs}
1	111	$\frac{1}{2}\frac{1}{2}\frac{3}{2}$	24	62	20	65	3	45
2	$20\bar{2}$	$0\bar{1}1$	7	11	10	14	6	17
	002	011	5	8	9	13	2	4
3	$33\bar{3}$	$\frac{3}{2}\frac{\bar{3}}{2}\frac{3}{2}$	1	4	3	4	16	18
	$22\bar{4}$	120	9	10	6	7	3	4
4	$60\bar{2}$	$0\bar{1}5$	9	15	7	10	4	8
	402	015	5	7	10	16	15	35
	133	$\frac{3}{2}\frac{3}{2}\frac{5}{2}$	16	24	11	19	0	1
5	$60\bar{3}$	$0\frac{\bar{3}}{2}\frac{3}{2}$	9	21	13	27	0	0
	$51\bar{1}$	$\frac{1}{2}\frac{1}{2}\frac{11}{2}$	10	23	5	15	11	33
6	$53\bar{1}$	$\frac{3}{2}\frac{\bar{1}}{2}\frac{3}{2}$	14	18	10	13	25	33
	313	$\frac{1}{2}\frac{3}{2}\frac{3}{2}$	7	9	5	6	4	5
7	$35\bar{1}$	$\frac{5}{2}\frac{1}{2}\frac{5}{2}$	6	8	15	23	2	6
	620	106	9	11	3	5	2	6
	$51\bar{5}$	$\frac{1}{2}\frac{\bar{5}}{2}\frac{5}{2}$	14	18	1	2	0	0
$R_I^* = \frac{\sum_i \lvert I_{obs} - I_{calc}\rvert}{\sum_i I_{obs}}$			42%		47%		57%	

TABLE V

CALCULATION OF MADELUNG SITE POTENTIALS (V) AND MADELUNG ENERGY (eV) FOR BOTH La_2NiO_4 (*Bmab* SPACE GROUP) AND $La_2NiO_{4.25}$ (*C*2 OR *Cm* SPACE GROUP) ON THE BASIS OF THE CLASSICAL CATIONIC AND ANIONIC CHARGE DISTRIBUTION (La^{3+}, Ni^{2+}, Ni^{3+}, O^{2-})

	Madelung Site Potentials (V)		
Atomic site	La_2NiO_4 Orthorhombic Bmab	$La_8Ni_4O_{17}$ Monoclinic *C*2	$La_8Ni_4O_{17}$ Monoclinic *Cm*
La	−28.06	−28.58	−28.59
Ni	−27.95	−31.58	−31.60
O_{xy}	21.41	22.98	23.08
O_z	20.00	19.37	19.22
O_I	—	13.25	6.08
Madelung energy (eV)	195.14	213.85[a]	211.90[a]

[a] This value is divided by 4 to compare with La_2NiO_4.

comparison between $\mathcal{R}$ and theoretical values (*15*, *16*) makes it possible to determine the significance level above which the hypothesis has to be ruled out.

In our case the obtained values led us to reject the *C*2/*m* hypothesis in comparison with *C*2 at the 0.1% significance level ($\mathcal{R}$ = 1.022 and $\mathcal{R}_{37,2794,0.001}$ = 1.024).

As far as the comparison between *C*2/*m* and *Cm* is concerned, the test is not significant (25% significance level ($\mathcal{R}$ = 1.0100 and $\mathcal{R}_{49,2782,0.25}$ = 1.0100).

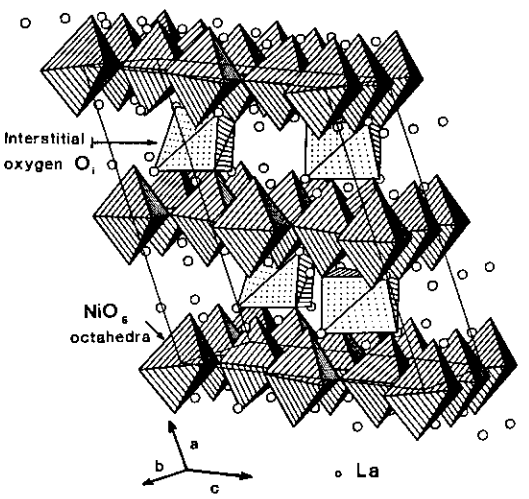

FIG. 8. Structure of the *C*2 monoclinic $La_8Ni_4O_{17}$ showing the ordering and the (La_4O_4) polyhedra of the interstitial oxygen atoms.

3. *Madelung Site Potential*

The results of the calculation of Madelung energy and site potentials using the Ewald methods (*17*) for both *C*2 and *Cm* space groups are reported in Table V.

The values of the O_I site potential are less important than those of O_{xy} and O_z sites for the two space groups. The very weak value of the O_I potential site in the *Cm* group leads us to consider the *C*2 group as the most likely. In addition, this space group gives the most stable lattice.

All these results lead to the conclusion that the most relevant space group is *C*2.

The results of the *C*2 structure refinement at 298 and 9 K are given in Table VI, a plot of the refinement profile is shown in Fig. 7, and the structure is plotted in Fig. 8.

The additional oxygen atoms are ordered to fully occupied sites leading to a definite new compound, $La_8Ni_4O_{17}$. The interstitial oxygen atoms O_I are surrounded by four La cations and four apical oxygen atoms (see discussion in Section II).

It should be pointed out that at 298 K the value of the temperature factor of the O_I oxygen is relatively high. This observation

TABLE VI

REFINED STRUCTURAL PARAMETERS FOR $La_8Ni_4O_{17}$ (C_2 SPACE GROUP) AT 300 K AND 9 K

	$La_8Ni_4O_{17}$, $C2$, 300 K a = 13.8326(3) Å b = 10.9300(2) Å c = 10.9125(2) Å β = 113°309(2)				$La_8Ni_4O_{17}$, $C2$, 9 K a = 13.7923(3) Å b = 10.9101(2) Å c = 10.8919(2) Å β = 113°320(2)			
Atoms	X	Y	Z	B(Å^2)	X	Y	Z	B(Å^2)
La(1)	0.636(1)	0.005(1)	0.822(1)	0.46(4)	0.639(1)	0.000(1)	0.821(1)	0.15(4)
La(2)	0.362(1)	0.006(1)	0.682(1)	0.46(4)	0.362(1)	−0.002(4)	0.680(1)	0.15(4)
La(3)	0.147(1)	0.002(1)	0.326(1)	0.46(4)	0.151(1)	0.005(1)	0.331(1)	0.15(4)
La(4)	0.865(1)	0.000	0.186(1)	0.46(4)	0.867(1)	0.000	0.184(1)	0.15(4)
La(5)	0.363(1)	0.248(1)	0.933(1)	0.46(4)	0.357(1)	0.245(4)	0.926(1)	0.15(4)
La(6)	0.639(1)	0.2500	0.567(1)	0.46(4)	0.631(1)	0.25	0.565(1)	0.15(4)
La(7)	0.147(1)	0.261(1)	0.078(1)	0.46(4)	0.142(1)	0.256(1)	0.075(1)	0.15(4)
La(8)	0.862(1)	0.255(1)	0.436(1)	0.46(4)	0.863(1)	0.249(1)	0.439(1)	0.15(4)
Ni(1)	0	0.001(1)	0	0.45(4)	0	0.007(1)	0	0.18(4)
Ni(2)	0	0.506(1)	0	0.45(4)	0	0.500(1)	0	0.18(4)
Ni(3)	0	0.003(1)	0.5	0.45(4)	0	−0.001(1)	0.5	0.18(4)
Ni(4)	0	0.505(1)	0.5	0.45(4)	0	0.500(1)	0.5	0.18(4)
Ni(5)	−0.006(1)	0.257(1)	0.744(1)	0.45(4)	0.005(1)	0.256(1)	0.748(1)	0.18(4)
Ni(6)	−0.004(1)	0.750(1)	0.253(1)	0.45(4)	0.000(1)	0.746(1)	0.256(1)	0.18(4)
O_{xy}(1)	−0.010(1)	0.130(1)	0.870(1)	0.51(5)	−0.023(1)	0.133(1)	0.858(1)	0.25(6)
O_{xy}(2)	0.500(1)	0.132(1)	0.880(1)	0.51(5)	0.493(1)	0.125(1)	0.875(1)	0.25(6)
O_{xy}(3)	−0.003(1)	0.381(1)	0.877(1)	0.51(5)	−0.006(1)	0.378(1)	0.875(1)	0.25(6)
O_{xy}(4)	0.488(1)	0.374(1)	0.873(1)	0.51(5)	0.496(1)	0.372(1)	0.877(1)	0.25(6)
O_{xy}(5)	−0.006(1)	0.126(1)	0.622(1)	0.51(5)	−0.010(1)	0.121(1)	0.618(1)	0.25(6)
O_{xy}(6)	0.486(1)	0.133(1)	0.617(1)	0.51(5)	0.504(1)	0.132(1)	0.631(1)	0.25(6)
O_{xy}(7)	0.013(1)	0.375(1)	0.636(1)	0.51(5)	0.008(1)	0.375(1)	0.631(1)	0.25(6)
O_{xy}(8)	0.486(1)	0.382(1)	0.615(1)	0.51(5)	0.495(1)	0.374(1)	0.622(1)	0.25(6)
O_z(1)	0.827(2)	−0.012(1)	0.915(2)	0.94(8)	0.823(2)	−0.019(1)	0.897(2)	0.74(8)
O_z(2)	0.173(2)	0.018(1)	0.599(2)	0.94(8)	0.175(2)	0.011(1)	0.600(2)	0.74(8)
O_z(3)	0.322(2)	0.008(1)	0.410(2)	0.94(8)	0.324(2)	0.015(1)	0.418(2)	0.74(8)
O_z(4)	0.674(2)	0.012(1)	0.084(2)	0.94(8)	0.674(2)	0.003(1)	0.080(2)	0.74(8)
O_z(5)	0.174(2)	0.256(1)	0.839(2)	0.94(8)	0.173(2)	0.254(1)	0.828(2)	0.74(8)
O_z(6)	0.831(2)	0.282(1)	0.689(2)	0.94(8)	0.832(2)	0.272(1)	0.657(2)	0.74(8)
O_z(7)	0.336(2)	0.288(1)	0.131(2)	0.94(8)	0.337(2)	0.286(1)	0.124(2)	0.74(8)
O_z(8)	0.673(2)	0.289(1)	0.314(2)	0.94(8)	0.672(2)	0.280(1)	0.316(2)	0.74(8)
O_i	0.741(3)	0.139(3)	0.754(3)	2.6(5)	0.743(3)	0.134(3)	0.754(3)	2.0(4)

Note. Numbers in parentheses are standard deviations in units of the last significant digit.

is characteristic of a site in which the calculated electronic density is too high. This value could be also related to the high mobility of additional oxygen atoms. Obviously at 9 K, the unit cell parameters and the Debye–Waller factors are lower than those at room temperature. Interatomic distances are reported in Table VII. In spite of the number of refined parameters, the $C2$ structure refinement leads to results consistent with the *Fmmm* structure refinements. The NiO distances are indeed less accurate but widely differentiated, showing in this way that nickel cations might have various electronic configurations.

Conclusion

Insertion of oxygen atoms in the oxide network of La_2NiO_4 leads for the $La_2NiO_{4.25}$ composition to a new compound in which the additional oxygen atoms are ordered.

TABLE VII

BOND DISTANCES IN $La_8Ni_4O_{17}$ (*Fmmm* AND *C*2 SPACE GROUPS)

		Fmmm	*C*2	
		298 K	298 K	9 K
		La polyhedron		
La(1)–O_{xy}	[10]	2.624(1)	2.51(2)–2.75(2)[a]	2.55(2)–2.68(2)[a]
La(1)–O_z		2.38(1)–2.50(2)[a]	2.37(2)–3.13(2)[a]	2.34(2)–3.17(2)[a]
La(1)–O_I		2.36(1)–2.41(1)[a]	2.37(3)	2.35(3)
La(1)–O		2.52	2.67	2.66
La(2)–O_{xy}		2.624(1)	2.51(2)–2.74(2)[a]	2.54(2)–2.67(2)[a]
La(2)–O_z	[9]	2.332(5)–2.768(5)[a]	2.42(2)–3.13(2)[a]	2.37(2)–3.11(2)[a]
La(2)–O		2.656	2.68	2.66
La(3)–O_{xy}	[10]	2.624(1)	2.54(2)–2.64(2)[a]	2.54(2)–2.78(2)[a]
La(3)–O_z		2.38(1)–2.50(2)[a]	2.22(2)–3.08(2)[a]	2.20(2)–2.92(2)[a]
La(3)–O_I		2.36(1)–2.41(1)[a]	2.54(3)	2.47(3)
La(3)–O		2.52	2.63	2.61
La(4)–O_{xy}	[9]	2.624(1)	2.62(2)–2.74(2)[d]	2.60(2)–2.78(2)[a]
La(4)–O_z		2.332(5)–2.768(5)[a]	2.43(2)–2.85(2)[a]	2.45(2)–2.95(2)[a]
La(4)–O		2.656	2.64	2.66
La(5)–O_{xy}	[9]	2.624(1)	2.52(2)–2.68(2)[a]	2.49(2)–2.68(2)[a]
La(5)–O_z		2.332(5)–2.768(5)[a]	2.33(2)–2.67(2)[a]	2.37(2)–2.66(2)[a]
La(5)–O		2.656	2.54	2.55
La(6)–O_{xy}	[10]	2.624(1)	2.43(2)–2.78(2)[a]	2.50(2)–2.58(2)[a]
La(6)–O_z		2.38(1)–2.50(2)[a]	2.49(2)–3.20(2)[a]	2.55(2)–3.25(2)[a]
La(6)–O_I		2.36(1)–2.41(1)[a]	2.32(3)	2.39(3)
La(6)–O		2.52	2.71	2.69
La(7)–O_{xy}	[10]	2.624(1)	2.59(2)–2.83(2)[a]	2.45(2)–2.88(2)[a]
La(7)–O_z		2.38(1)–2.50(2)[a]	2.45(2)–3.00(2)[a]	2.54(2)–3.04(2)[a]
La(7)–O_I		2.36(1)–2.41(1)[a]	2.30(3)	2.33(3)
La(7)–O		2.52	2.65	2.69
La(8)–O_{xy}	[9]	2.624(1)	2.51(2)–2.70(2)[a]	2.48(2)–2.73(2)[a]
La(8)–O_z		2.332(5)–2.768(5)[a]	2.45(2)–2.97(2)[a]	2.45(2)–2.93(2)[a]
La(8)–O		2.656	2.68	2.65
		Ni octahedron		
			1.93(1) × 2	1.98(1) × 2
Ni(1)–O_{xy}		1.9306(1) × 4	1.96(1) × 2	2.00(1) × 2
Ni(1)–O_z		2.19(1) × 2	2.20(1) × 2	2.27(1) × 2
Ni(1)–O		2.02	2.03	2.08
			1.90(1) × 2	1.88(1) × 2
Ni(2)–O_{xy}		1.9306(1) × 4	1.90(1) × 2	1.90(1) × 2
Ni(2)–O_z		2.242(3) × 2	2.21(1) × 2	2.20(1) × 2
Ni(2)–O		2.035	2.00	1.99
			1.89(1) × 2	1.89(1) × 2
Ni(3)–O_{xy}		1.9306(1) × 4	1.91(1) × 2	1.92(1) × 2
Ni(3)–O_z		2.242(3) × 2	2.20(1) × 2	2.23(1) × 2
Ni(3)–O		2.03	2.00	2.01
			1.95(1) × 2	1.94(1) × 2
Ni(4)–O_{xy}		1.9306(1) × 4	2.01(1) × 2	2.01(1) × 2
Ni(4)–O_z		2.19(1) × 2	2.26(1) × 2	2.23(1) × 2
Ni(4)–O		2.02	2.08	2.06
Ni(5)–O_{xy}		1.9306(1) × 4	1.85(2)	1.84(2)
			1.96(2)	1.94(2)
			1.97(2)	1.97(2)
			1.98(2)	2.00(2)

(*Continued*)

TABLE VII—*Continued*

	Fmmm	*C2*	
	298 K	298 K	9 K
	2.19(1) × 2	2.10(2)	2.13(2)
$Ni(5)–O_z$	2.242(3)	2.29(2)	2.20(2)
Ni(5)–O	2.035	2.03	2.01
$Ni(6)–O_{xy}$	1.9306(1) × 4	1.85(2)	1.77(2)
		1.96(2)	1.91(2)
		1.99(2)	1.98(2)
		2.01(2)	2.01(2)
	2.19(1)	2.13(2)	2.18(2)
$Ni(6)–O_z$	2.242(3)	2.31(2)	2.23(2)
Ni(6)–O	2.03	2.04	2.01
	Environment of O_I(Å)		
$O_I–O_{xy}$		3.17(4)	2.97(4)
		3.24(4)	3.02(4)
$O_I–O_z$		2.18(5)	2.18(5)
		2.36(5)	2.25(5)
		2.29(5)	2.43(5)
		2.54(5)	2.62(5)
O_I–La		2.30(3)	2.33(3)
		2.38(3)	2.35(3)
		2.32(3)	2.43(3)
		2.54(3)	2.47(3)

Note. Numbers in parentheses are standard deviations in units of the last digit.
[a] Only the ranges of distances have been reported.

The electron diffraction study has revealed a C-centered monoclinic lattice with a unit cell four times bigger than the average orthorhombic unit cell previously proposed.

The Rietveld structure refinement was carried out on the basis of neutron powder diffraction data collected at 298 and 9 K. On the basis of the profile analysis, Hamilton's test, and calculations of the Madelung site potentials the C_2 space group appears as most relevant for describing the structure.

A detailed discussion of the nature of the additional oxygen atoms and the electronic configuration of the nickel atoms is reported in the second publication in this series and discussed in correlation with EPR and magnetic susceptibility measurements.

Acknowledgments

The authors acknowledge Dr. J. Darriet for fruitful discussion, J. L. Soubeyroux for the neutron experiments, and the Rhône-Poulenc Company for financial support.

References

1. J. Beille, R. Cabanal, C. Chaillout, B. Chevalier, G. Demazeau, F. Deslandes, J. Etourneau, P. Lejay, C. Michel, J. Provost, B. Raveau, A. Sulpice, J. L. Tholence, and R. Tournier, *C.R. Acad. Sci. Paris Ser. 2* **304,** 1097 (1987).
2. A. Wattiaux, J. C. Park, J. C. Grenier, and M. Pouchard, *C.R. Acad. Sci. Paris Ser. 2* **310,** 1047 (1990).
3. J. E. Schirber, B. Morosin, R. M. Merrill, P. F. Hlava, E. L. Venturini, J. F. Kwak, P. J. Nigrey, R. J. Baughmann, and D. G. Ginley, *Physica C* **152,** 121 (1988).
4. J. Zhou, S. Sinha, and J. B. Goodenough, *Phys. Rev. B* **39,** (16), 12,331 (1989).
5. J. D. Jorgensen, B. Dabrowski, S. Pei, D. R. Richards, and D. G. Hinks, *Phys. Rev. B* **40,** 2187 (1989).
6. T. Freltoft, D. J. Buttrey, G. Aeppli, D. Vaknin and G. Shirane, *Phys. Rev. B* **44** (10), 5046 (1991).
7. C. Chaillout, S. N. Cheong, Z. Fisk, M. S. Lehmann, M. Marezio, B. Morosin, and J. E. Schiber, *Physica C* **158,** 183 (1989).
8. Z. Hiroi, T. Obaka, M. Takano, Y. Bando, Y.

TAKEDA, AND O. YAMAMOTO, *Phys. Rev. B* **41,** 11,665 (1990).

9. A. DEMOURGUES, F. WEILL, J. C. GRENIER, A. WATTIAUX, AND M. POUCHARD, *Physica C* **192,** 425 (1992).
10. L. C. OTTERO-DIAZ, A. R. LANDA, F. FERNANDEZ, R. SAEZ-PUCHE, R. WITHERS, AND B. G. HYDE, *J. Solid State Chem.* **97,** 443 (1992).
11. A. WATTIAUX, L. FOURNÈS, A. DEMOURGUES, N. BERNABEN, J. C. GRENIER, AND M. POUCHARD, *Solid State Commun.* **77,** 489 (1991).
12. A. DEMOURGUES, A. WATTIAUX, J. C. GRENIER, M. POUCHARD, J. M. DANCE, J. L. SOUBEYROUX, AND P. HAGENMULLER, submitted for publication.
13. J. RODRIGUEZ-CARVAJAL, M. T. FERNANDEZ-DIAZ, AND J. L. MARTINEZ, *J. Phys. Condensed Matter* **3,** 3215 (1991).
14. A. DEMOURGUES, A. WATTIAUX, J. C. GRENIER, J. P. DOUMERC, P. DORDOR, E. MARQUESTAUT, AND M. POUCHARD, to be published.
15. W. C. HAMILTON, *Acta Crystallogr.* **18,** 502 (1965).
16. G. S. PAWLEY, *Acta Crystallogr. Sect. A.* **26,** 691 (1990).
17. P. P. EWALD, *Ann. Phys.* **64,** 253 (1921).